3-Hydroxyterphenyllin, a natural fungal metabolite, induces apoptosis and S phase arrest in human ovarian carcinoma cells

YAOMIN WANG[1,2], CASEY COMPTON[2], GARY O. RANKIN[3], STEPHEN J. CUTLER[4], YON ROJANASAKUL[5], YOUYING TU[1] and YI CHARLIE CHEN[2]

[1]Department of Tea Science, Zhejiang University, Hangzhou, Zhejiang 310058, P.R. China; [2]College of Science, Technology and Mathematics, Alderson Broaddus University, Philippi, WV 26416; [3]Department of Biomedical Sciences, Joan C. Edwards School of Medicine, Marshall University, Huntington, WV 25755; [4]Department of BioMolecular Sciences, University of Mississippi, University, MS 38677; [5]Department of Pharmaceutical Sciences, West Virginia University, Morgantown, WV 26506, USA

Received December 30, 2016; Accepted February 13, 2017

DOI: 10.3892/ijo.2017.3894

Abstract. In the present study, we evaluated 3-Hydroxyterphenyllin (3-HT) as a potential anticancer agent using the human ovarian cancer cells A2780/CP70 and OVCAR-3, and normal human epithelial ovarian cells IOSE-364 as an *in vitro* model. 3-HT suppressed proliferation and caused cytotoxicity against A2780/CP70 and OVCAR-3 cells, while it exhibited lower cytotoxicity in IOSE-364 cells. Subsequently, we found that 3-HT induced S phase arrest and apoptosis in a dose-independent manner. Further investigation revealed that S phase arrest was related with DNA damage which mediated the ATM/p53/Chk2 pathway. Downregulation of cyclin D1, cyclin A2, cyclin E1, CDK2, CDK4 and Cdc25C, and the upregulation of Cdc25A and cyclin B1 led to the accumulation of cells in S phase. The apoptotic effect was confirmed by Hoechst 33342 staining, depolarization of mitochondrial membrane potential and activation of cleaved caspase-3 and PARP1. Additional results revealed both intrinsic and extrinsic apoptotic pathways were involved. The intrinsic apoptotic pathway was activated through decreasing the protein levels of Bcl2, Bcl-xL and procaspase-9 and increasing the protein level of Puma. The induction of DR5 and DR4 indicated that the extrinsic apoptotic pathway was also activated. Induction of ROS and activation of ERK were observed in ovarian cancer cells. We therefore concluded that 3-HT possessed anti-proliferative effect on A2780/CP70 and OVCAR-3 cells, induced S phase arrest and caused apoptosis. Taken together, we propose that 3-HT shows promise as a therapeutic candidate for treating ovarian cancer.

Correspondence to: Dr Yi Charlie Chen, College of Science, Technology and Mathematics, Alderson Broaddus University, 101 College Hill Drive, Philippi, WV 26416, USA
E-mail: chenyc@ab.edu

Dr Youying Tu, Department of Tea Science, Zhejiang University, 866 Yuhangtang Road, Hangzhou, Zhejiang 310058, P.R. China
E-mail: youytu@zju.edu.cn

Key words: 3-Hydroxyterphenyllin, apoptosis, DNA damage, ovarian cancer, S phase arrest

Introduction

Epithelial ovarian cancer is the fifth most common cause of cancer-related death among women in the United States. Though more than 80% of patients with advanced ovarian cancer benefit from first-line therapy, 75% of those patients will experience tumor recurrence due to widespread metastasis within the abdomen (1,2). The current available treatments for ovarian cancer include tumor debulking surgery and chemotherapy. Cisplatin is an important chemotherapeutic drug for the treatment of ovarian cancer. However, the majority of patients who respond to cisplatin initially will relapse due to the development of resistance (3). Thus, there is an urgent need to search for new agents derived from naturally occurring secondary metabolites. Since the 1940s, 175 small molecule cancer drugs have been developed. A total of 131 of those drugs are considered 'other than synthetic' and 85 drugs are natural products or their direct derivitives which are mainly derived from bacteria and plants (4). In recent years, more attention has been paid to fungi-derived natural products which have promising anticancer activities. Many fungal metabolites have demonstrated notable *in vitro* growth-inhibitory properties against various human cancer cell lines. Moreover, selected metabolites have exhibited therapeutic benefits *in vivo* mouse models (5). 3-Hydroxyterphenyllin (3-HT; Fig. 1A), is a metabolite isolated from *Aspergillus candidus*. The compound was first discovered in 1979 (6). It effectively inhibited the development of sea urchin embryonic development (7). The inhibitory pattern 3-HT exhibited was similar to Candidusin B, which is also isolated from *Aspergillus candidus* and could suppress DNA and RNA syntheses in embryos. Other reports suggested that 3-HT possessed antioxidative properties and showed neither cytotoxic nor genotoxic traits against human intestine 470 cells (INT 470); though, it showed protective effects

against oxidative damage to INT 407 cells (8,9). However, the anticancer effects of 3-HT have not been investigated.

In the present study, we investigated the anticancer effect of 3-HT. Currently, it has been proven that apoptosis is an important biological pathway of programmed cell death in multicellular organisms, promoting apoptosis has become a key strategy for cancer drug discovery (10). Targeting the apoptosis signal transduction pathway has become pivotal in the implication for cancer therapy (11). Also, inducing cell cycle arrest is an effective way to restrict tumor growth *in vitro* and *in vivo*. We have previously reported that Chaetoglobosin K, a secondary metabolite isolated from the fungus *Diplodia macrospora*, could induce apoptosis and G2 cell cycle arrest in ovarian cancer cells (12). Other reports have also proven that metabolites isolated from marine-derived fungal metabolites could induce apoptosis or cell cycle arrest in different human cancer cell lines (13,14). All these studies provide a promising prospect for discovering anticancer drugs from fungal metabolites.

Therefore, considering the lack of published reports on the anticancer effects of 3-HT in human cancer cells, we aimed to investigate its anticancer effects and the molecular signaling pathway using two ovarian cancer cell lines, A2780/CP70 and OVCAR-3, and a normal human epithelial ovarian cell line, IOSE-364 as *in vitro* models. Our results demonstrate that 3-HT has effective anticancer effect and provide foundations for further studies.

Materials and methods

Materials. 3-Hydroxyterphenyllin (3-HT), was obtained from the Cutler Laboratory (University of Mississippi, Oxford, MS, USA). 3-HT was dissolved in dimethyl sulfoxide (DMSO) to a concentration of 10 mM and stored at -20˚C. Working concentrations of 0, 2, 4, 8, 12 and 16 μM, as for control, DMSO was diluted by cell culture medium at a final concentration that was equal to the maximal concentration of the 3-HT solvent. RPMI-1640 medium, bovine serum albumin (BSA), DMSO, Hoechst 33342 and DCFH-DA were purchased from Sigma-Aldrich (St. Louis, MO, USA). Fetal bovine serum (FBS), phosphate-buffered saline (PBS) and propidium iodide (PI) were purchased from Life Technologies (Grand Island, NY, USA). CellTiter 96® AQ_{ueous} One Solution Cell Proliferation assay was purchased from Promega (Madison, WI, USA). Pierce LDH Cytotoxicity assay kit and Alexa Fluor® 488 Annexin V/Dead Cell Apoptosis kit were purchased from Thermo Fisher Scientific (Waltham, MA, USA). Primary antibodies to caspase-3, caspase-9, p21Waf1/Cip1 (12D1), p38, Bax, Bcl-2, Puma, FADD, cyclin B1, cyclin A2, cyclin D1, cyclin E1, CDK2, CDK4, cdc2, cdc25c, cdc25A, p-ATM (Ser1981), ATM, DR5, Fas and γ-H2AX (Ser139) were purchased from Cell Signaling Inc. (Danvers, MA, USA). Primary antibodies to p53 (C11), p-p53 (Ser15), PARP-1 (F-2), Bad (C-7), Bcl-xL (H-5), p-ERK1/2 (Thr202), ERK1 (K-23), chk1 (G4), p-chk2 (Thr68), chk2 (H-300), DR4 (H-130), GAPDH (0411) and the secondary antibodies were purchased from Santa Cruz Biotechnology (Santa Cruz, CA, USA).

Cell lines and cell culture. The human ovarian carcinoma cell lines, A2780/CP70 and OVCAR-3 were provided by Dr Jiang from the West Virginia University, the normal ovarian surface epithelial cell line IOSE-364 was provided by Dr Auersperg from the University of British Columbia. All cell lines were cultured in RPMI-1640 medium, supplemented with 10% FBS, and incubated in a humidified incubator with 5% CO_2 at 37˚C.

Cell viability assay. The effect of 3-HT on cell viability was measured by the CellTiter 96® AQ_{ueous} One Solution Cell Proliferation assay. A total of $1.0x10^4$ cells/well were seeded in 96-well plates. After incubation for 24 h, the cells were treated with different concentrations of 3-HT for 24 h and then 100 μl AQ_{ueous} One reagent was added to each well and incubated for another 1 h. Absorbance was measured at 490 nm using a microplate reader (Synergy™ Multi-Mode; BioTek Instruments, Inc., Winooski, VT, USA). Cell viability was expressed as a percentage of control.

LDH cytotoxicity assay. LDH assay was determined by LDH cytotoxicity assay kit according to the manufacturer's guidelines. Briefly, cells were seeded in 96-well plates with the density of $1x10^4$ cells/well. After a 24-h growth period, cells were exposed to 3-HT at different concentrations for 24 h. After incubation, lysis buffer and reaction mixture were added to the wells according to the manufacturer's instruction. The absorbance at 490 and 680 nm was detected by the microplate reader. LDH cytotoxicity was calculated using the following formula:

$$\% \text{ Cytotoxicity} = \frac{\text{(Compound-treated LDH activity - spontaneous LDH activity)}}{\text{(Maximum LDH activity - spontaneous LDH activity)}} \times 100$$

Cell cycle analysis. Cell cycle distribution of 3-HT-treated cells was determined by flow cytometric analysis. Briefly, A2780/CP70 and OVCAR-3 cell were incubated at a density of ~$1x10^5$ cells/well. After exposing with 3-HT at different concentrations for 24 h, cells were washed twice with PBS and fixed with ice-cold 70% ethanol at 4˚C overnight. The fixed cells were washed twice with PBS followed by incubation with RNase A (180 μg/ml) for 30 min at 37˚C. After incubation with PI solution (final concentration 50 μg/ml) for another 30 min in the dark, cell cycle analysis was performed by FACSCalibur flow cytometry system (BD Biosciences, San Jose, CA, USA). A total of 20,000 cells of each sample were recorded for the analysis. Results were processed by FCS Software (De Novo Software, Los Angeles, CA, USA).

Hoechst 33342 staining for apoptosis analysis. Hoechst 33342, a blue fluorescent dye, was used to analyze the apoptotic effect. Briefly, ~$1x10^4$ cells/well were seeded in 96-well plates. After 24-h incubation, cells were treated with (0, 2, 4 and 8 μM) 3-HT for 24 h, then washed with PBS and stained with 10 μg/ml of Hoechst 33342 in PBS for 15 min at 37˚C. After that, cells were assessed by fluorescence microscopy (Carl Zeiss, Heidelberg, Germany) in a blinded manner to avoid experimental bias. Apoptotic effect was evaluated through morphological changes.

Analysis of apoptosis by flow cytometry. Induction of apoptosis was detected using Alexa Fluor® 488 Annexin V/Dead Cell

Apoptosis kit according to the manufacturer's protocol. Briefly, after treatment with 3-HT for 24 h, cells were harvested and washed twice with cold PBS. The cells were then suspended in 100 μl Annexin-binding buffer and stained by adding 5 μl Annexin V-fluorescein isothiocyanate and 1 μl 100 μg/ml PI solution for 15 min in the dark at room temperature. Next 400 μl of Annexin-binding buffer was added to each sample. Subsequently, 10,000 events of each sample were analyzed using flow cytometry within 1 h (BD Biosciences).

Measurement of mitochondrial membrane potential ($\Delta\Psi m$). The mitochondrial membrane potential was measured by JC-1 staining (Invitrogen). Cells were treated with (0, 2, 4 and 8 μM) 3-HT for 24 h, then washed twice with PBS followed by incubation with 10 μg/ml JC-1 for 30 min in an incubator with 5% CO_2 at 37˚C. The fluorescence intensity of red to green was then measured with a fluorescence plate reader at excitation: emission of 485/595 and excitation: emission of 485/535, respectively.

Western blot analysis. Cells were treated with 3-HT at different concentrations for 24 h. Total protein was extracted by M-PER® mammalian protein extraction reagent supplemented with 1% Halt™ Protease Inhibitor Single-Use Cocktail on ice for 30 min. The protein concentration was measured using BCA protein assay kit. Equal amounts of protein were separated electrophoretically with SDS-PAGE gels and transferred to nitrocellulose membranes using Mini-PROTEAN 3 system (Bio-Rad Laboratories, Hercules, CA, USA). The membrane was blocked with 5% non-fat milk for 1 h and followed by incubating with specific primary antibodies at 4˚C overnight. Membranes were washed in TBST three times for 30 min, then were incubated with secondary antibodies for 2 h at room temperature. Secondary antibodies were removed through washing the membranes in TBST three times for 30 min. The membranes were then exposed in SuperSignal® West Pico Luminol Enhancer Solution (Thermo Fisher Scientific, Rockford, IL, USA) for 10 min. The visualization of protein bands was performed by ChemiDoc™ MP System (Bio-Rad Laboratories). Protein bands were quantified using NIH ImageJ software and protein levels were normalized by GAPDH as internal control.

Intracellular ROS measurement. Peroxide-sensitive fluorescent probe DCFH-DA was used to detect the intracellular ROS production. Cells were treated with (0, 2, 4 and 8 μM) 3-HT for 24 h and then incubated with DCFH-DA (10 μM) for 30 min at 37˚C. After staining with DCFH-DA, the fluorescence intensity was measured by microplate reader with excitation at 485 nm and emission at 528 nm. Total protein level was detected to normalize the ROS generation; the results were expressed as percentage of control.

Statistical analysis. All data were presented as mean ± SEM of at least three independent experiments. Statistical analysis was performed by Graphpad Prism software and statistical comparison was evaluated by one-way analysis of variance with Newman-Keuls test. The significant differences were shown as $P<0.05$, $P<0.01$ and $P<0.001$.

Results

3-HT suppresses cell growth and induces cytotoxicity of ovarian cancer cells. We used cell lines A2780/CP70, OVCAR-3 and IOSE-364 to investigate the effect of 3-HT on ovarian cancer cells. As shown in Fig. 1C, 3-HT substantially suppressed ovarian cancer cell growth in a dose-dependent manner, especially in high doses (12 and 16 μM). In contrast, 3-HT displayed relatively moderate cytotoxicity toward normal ovarian surface epithelial cell line IOSE-364 (Fig. 1C). To further explore the cytotoxicity effect of 3-HT on IOSE-364, A2780/CP70 and OVCAR-3 cells, LDH assay was assessed after treatment with 3-HT at different concentrations for 24 h. As shown in Fig. 1B, no significant variations were observed at concentrations ranging from 2 to 8 μM while a dramatic increase in LDH release was observed at 12 μM in both A2780/CP70 and OVCAR-3 cells. 3-HT slightly induced LDH release in IOSE-364 cells, which meant that 3-HT caused less cytotoxicity in normal ovarian cells than in cancer cells. Taken together, the results indicated that 3-HT exhibited a growth inhibitory effect and cytotoxicity on both A2780/CP70 and OVCAR-3 cells in a dose-dependent manner.

3-HT triggers cell cycle arrest at the S phase. We hypothesized that the reduced cell viability and increased cytotoxicity after treatment with 3-HT might occur due to the inhibition of cell progression. To further demonstrate this hypothesis, we determined the effect of 3-HT on cell cycle arrest. After treatment with 3-HT at various concentrations (0, 2, 4 and 8 μM) for 24 h, the percentages of G0/G1, S and G2/M phase-specific cells were evaluated and plotted. We observed significant accumulation of cells in S phase in a dose-dependent manner in both A2780/CP70 (Fig. 2A) and OVCAR-3 cells (Fig. 2B). Compared with the control group, the percentages of 3-HT-treated A2780/CP70 cells at 2, 4 and 8 μM in the S phase increased from 35.75±0.231 to 68.91±7.885, 73.28±0.749 and 79.37±0.499%, respectively (Fig. 2C). Similarly, the percentages of 3-HT-treated OVCAR-3 cells at 2, 4 and 8 μM in the S phase increased from 32.28±0.745 to 68.91±1.220, 73.28±0.612 and 79.37±1.258%, respectively (Fig. 2D). In addition, a decrease in both G0/G1 and G2/M cell populations occurred concomitant with the increase in S phase. These results revealed that 3-HT induced S phase arrest in both ovarian cancer cell lines.

3-HT induces apoptosis of ovarian cancer cells. Based on the results that 3-HT could induce S phase arrest in ovarian cancer cells, we next probed whether 3-HT caused apoptosis. We used Hoechst 33342 staining to assess 3-HT-induced changes in nuclear morphology. As shown in Fig. 3A, A2780/CP70 and OVCAR-3 cells treated with 3-HT for 24 h exhibited dramatic nuclear morphology changes. Typical apoptotic nuclear morphology such as nuclear shrinkage, fragmentation and condensation were observed (Fig. 3A). We next investigated the pro-apoptotic effect by using flow cytometric analysis via Annexin V/PI staining. The results showed that 3-HT-treated OVCAR-3 cells underwent significant apoptosis in a dose-dependent manner (Fig. 3C). The apoptotic rate increased to 31.3% at 8 μM in OVCAR-3 cells vs. 5.8% in the control group (Fig. 3E). Though there was no significant difference

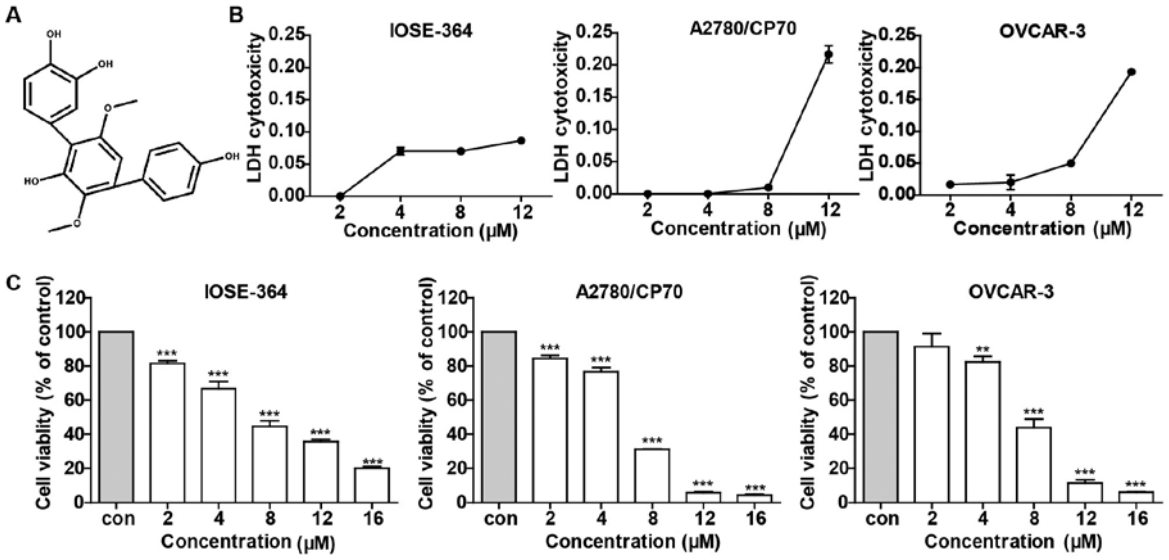

Figure 1. 3-HT causes cytotoxicity and reduces cell viability in A2780/CP70 and OVCAR-3 cells, while has limited effect on IOSE-364 cells. (A) The chemical structure of 3-Hydroxyterphenyllin. (B) LDH cytotoxicities of 3-HT on IOSE-364, A2780/CP70 and OVCAR-3 cells were determined by LDH assay after treatment at indicated concentrations (0, 2, 4, 8 and 12 μM) for 24 h. (C) Effect of 3-HT on cell viability of A2780/CP70, OVCAR-3 and IOSE-364 cells was assayed using the MTS method after treatment with various concentrations of 3-HT for 24 h. Data were expressed as mean ± SEM of triplicate experiments. **P<0.01 and ***P<0.001.

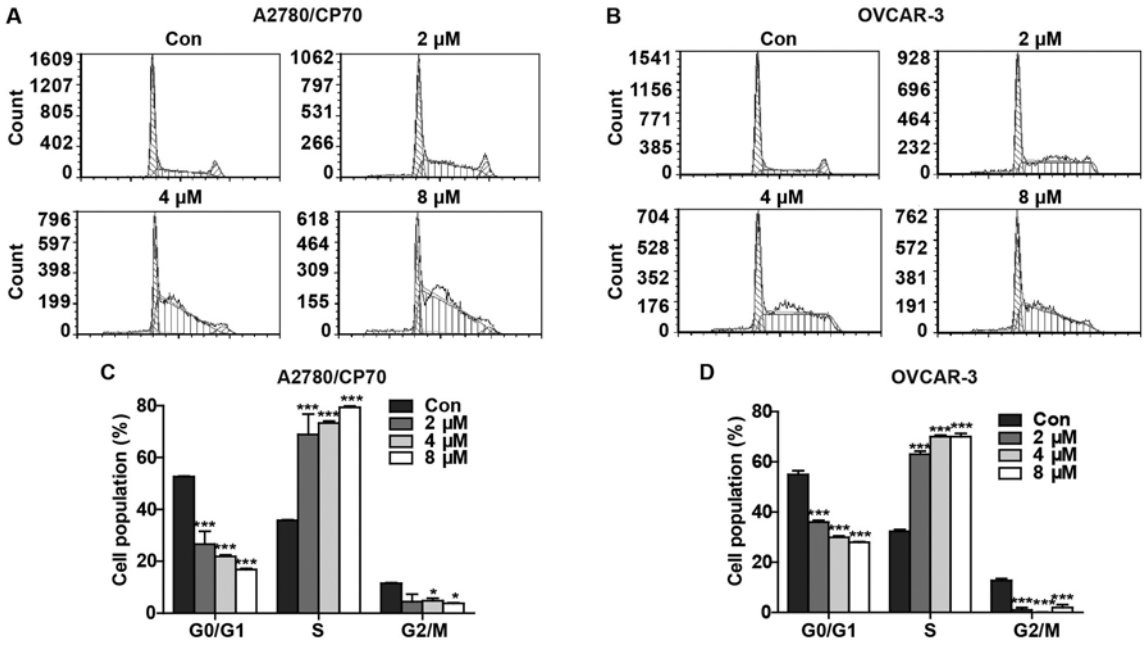

Figure 2. 3-HT induces cell cycle arrest in A2780/CP70 and OVCAR-3 cells. (A and B) Cell cycle distributions of A2780/CP70 cells and OVCAR-3 cells. Cells were treated with 3-HT (0, 2, 4 and 8 μM) for 24 h, followed by fixing in 70% methanol, and then stained with propidium iodide, cell cycle distributions were conducted by flow cytometric analysis. (C and D) A2780/CP70 and OVCAR-3 cell cycle distribution data were expressed as means ± SEM of three independent experiments. *P<0.05, ***P<0.001.

of apoptotic rate in A2780/CP70 cells (Fig. 3D), we observed a growth trend of apoptosis rate as the concentration of 3-HT increased (Fig. 3B).

Loss of mitochondrial membrane potential is considered a hallmark of apoptosis. To further confirm that 3-HT induced apoptosis, the mitochondrial membrane potential of A2780/CP70 and OVCAR-3 cells was measured after treatment with 3-HT at 0, 2, 4 and 8 μM for 24 h. The JC-1 fluorescence ratio (red/green) decreased markedly in both ovarian cancer cells (Fig. 3F and G), which suggested that depolarization of mitochondrial membrane potential and apoptosis occurred. Furthermore, apoptosis-related proteins were also evaluated by western blot analysis. As expected, treatment with increasing concentrations of 3-HT for 24 h significantly decreased the procaspase-3 levels in both A2780/CP70 and OVCAR-3 cells (Fig. 3H) and simultaneously increased the cleaved caspase-3 level in A2780/CP70 cells (Fig. 3H). The 89-kDa cleaved PARP fragments were detected

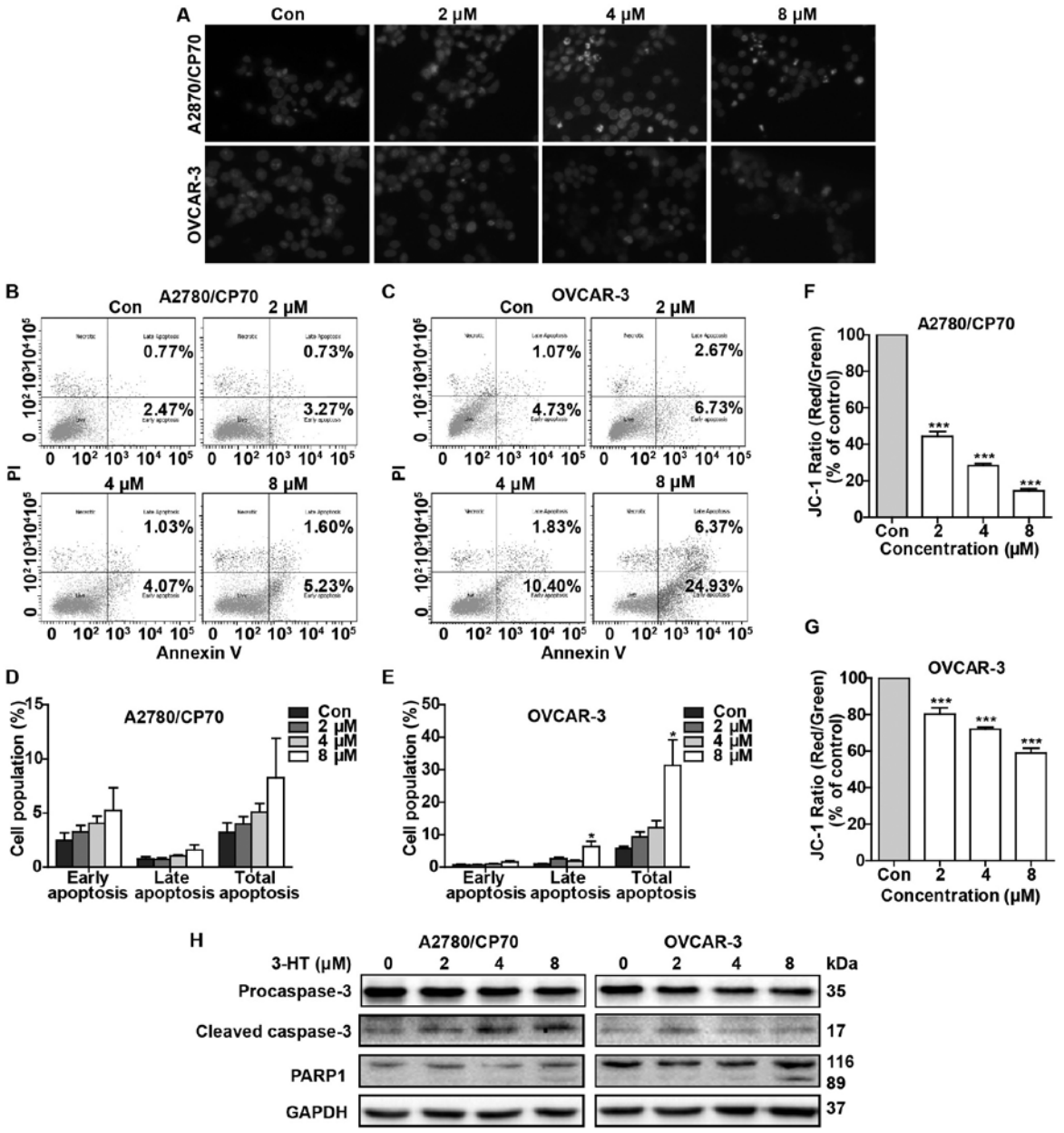

Figure 3. 3-HT induces apoptosis in A2780/CP70 and OVCAR-3 cells. (A) Hoechst 33342 staining was conducted in the experiment. A2780/CP70 and OVCAR-3 cells were treated with 3-HT for 24 h, stained with Hoechst 33342, and then detected by fluorescent microscopy (magnification, x400). (B) Flow cytometric analysis of A2780/CP70 cells and (C) OVCAR-3 cells. Cell were treated with 3-HT for 24 h, then stained with Annexin V-FITC and PI solution and analyzed with flow cytometry. (D and E) Apoptosis data were expressed as mean ± SEM of three independent experiments; *P<0.05. (F and G) Mitochondrial membrane potential changes of A2780/CP70 and OVCAR-3 cells were determined using JC-1. Cells were treated with 3-HT for 24 h and stained with JC-1, the fluorescence intensity of red to green was measured by fluorescence microplate reader. Data were expressed as mean ± SEM of three independent experiments; ***P<0.001. (H) Protein expression levels of procaspase-3, cleaved caspase-3 and PARP1 were analysed by western blotting. A2780/CP70 and OVCAR-3 cells were treated with 3-HT for 24 h, the cell lysates were then prepared for western blot analysis. GAPDH was used as internal control.

in both cell types at a high concentration (8 μM) of 3-HT (Fig. 3H). Together, these results demonstrated that 3-HT can induce apoptosis in ovarian cancer cells.

3-HT induces S phase arrest related with DNA damage. DNA damage can lead to S phase arrest and result in DNA damage repair response (15). To determine whether 3-HT induces DNA damage in ovarian cancer cells, we evaluated changes of the protein levels of γ-H2AX (Ser139), p-ATM, ATM, Chk1/2, p53, p-p53 (Ser15), p21 and Cdc25C after treatment with 3-HT for 24 h. The phosphorylation of H2AX at Ser139 indicates DNA double-strand breaks. ATM, another sensor of DNA damage, is phosphorylated after DNA damage (16). Results showed a dramatic increase of γ-H2AX at Ser-139 in both 3-HT treated ovarian cancer cells (Fig. 4A-C). Additionally, the expression of p-ATM significantly increased at the concentration of 8 μM compared with control in A2780/CP70 cells (Fig. 4A and B). The phosphorylation of ATM can phosphorylate Chk1 and Chk2 which are considered key downstream checkpoint substrates of ATM, thus, leading to cell cycle arrest. Treatment with 3-HT resulted in significant increase of the phosphorylation of Chk2 (Thr68) in a dose-dependent

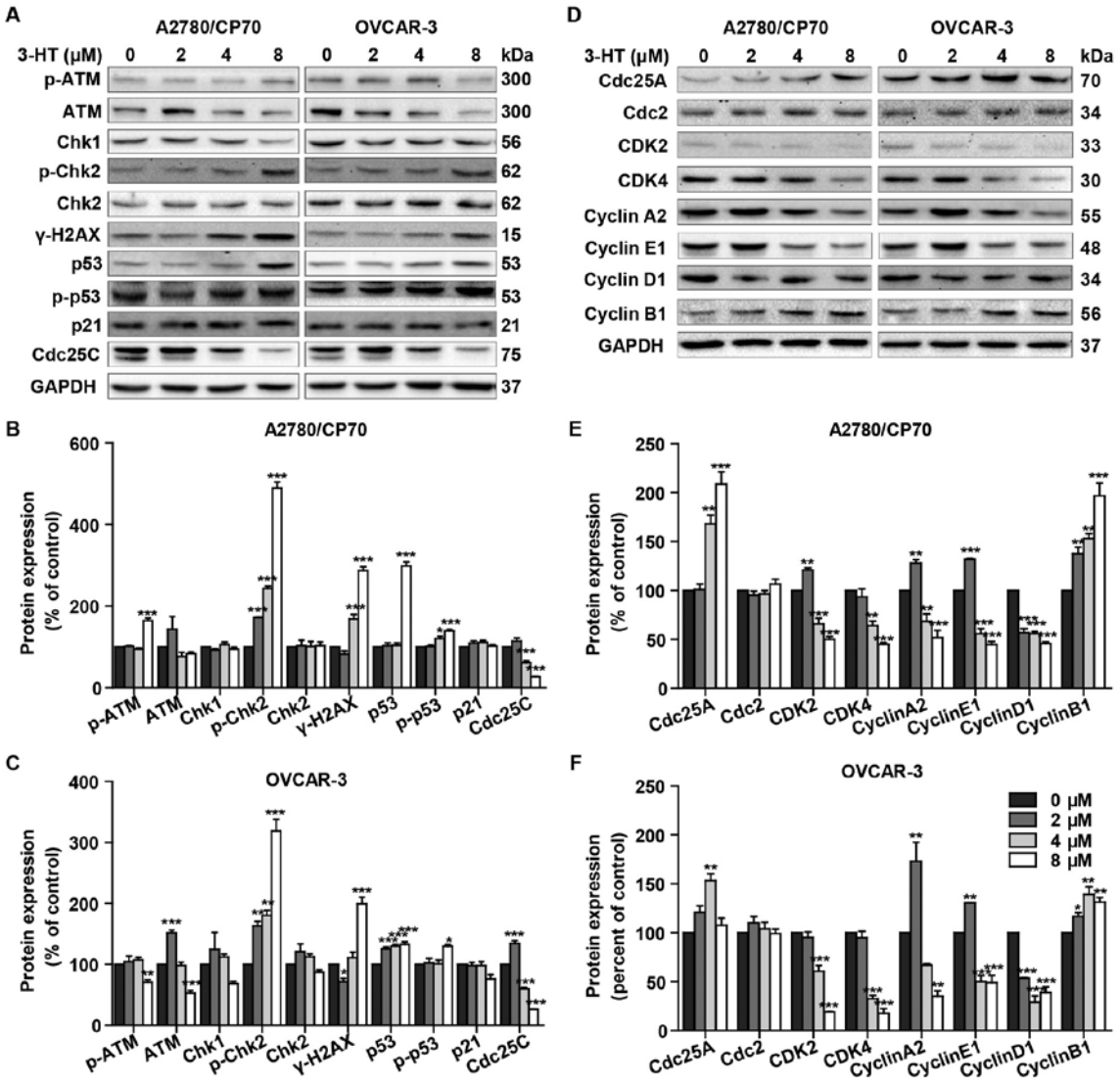

Figure 4. Effect of 3-HT on DNA damage and cell cycle regulatory proteins in A2780/CP70 and OVCAR-3 cells. (A) The DNA damage regulatory proteins in A2780/CP70 and OVCAR-3 cells were detected by western blotting, cells were incubated with 3-HT at 0-8 μM for 24 h, cell lysates were prepared and then subjected to western blotting, GAPDH was used as internal control. (B and C) A2780/CP70 and OVCAR-3 protein expression data were expressed as means ± SEM of three independent experiments. *P<0.05, **P<0.01, ***P<0.001. (D) The cell cycle regulatory proteins in A2780/CP70 and OVCAR-3 cells were detected by western blotting, cells were incubated with 3-HT at 0-8 μM for 24 h, cell lysates were prepared and then subjected to western blotting, GAPDH was used as internal control. (E and F) A2780/CP70 and OVCAR-3 protein expression data were expressed as means ± SEM of three independent experiments. *P<0.05, **P<0.01, ***P<0.001.

manner in A2780/CP70 and OVCAR-3 cells (Fig. 4A-C). Chk1 decreased while Chk2 remained unchanged in both cells (Fig. 4A-C). We concluded that 3-HT-induced DNA damage involved the activation of ATM-Chk2 pathways. A target of DNA damage-induced phosphorylation is p53 protein. DNA damage results in phosphorylation on Ser15 of p53 (17). Western blotting results indicated that 3-HT exposure increased phosphorylation of p53 (Ser15) and p53 total protein levels in both ovarian cancer cell lines (Fig. 4A-C). Whereas, the downstream protein Cdc25C was downregulated while p21 remained unchanged (Fig. 4A-C).

To further investigate the mechanism of 3-HT-induced S phase arrest, we then evaluated the expression of cell cycle-regulatory proteins, such as cyclins, cyclin-dependent kinases (CDKs), and cell division cycle (Cdc) proteins using western blotting. Our results showed a dramatic downregulation in protein levels of CDK2, CDK4, cyclin E1, cyclin A2 and cyclin D1, while the protein levels of Cdc25A and cyclin B1 were upregulated (Fig. 4D-F). Cdc2 remained unchanged in both cancer cell types (Fig. 4D-F). Taken together, these results indicated that 3-HT induced S phase arrest through regulation of the expression of the cell cycle proteins.

3-HT induces ROS accumulation and activates the MAPK signaling pathway. Since many anticancer compounds could induce ROS generation and activate MAPK signaling pathway ultimately causing apoptosis, we then examined the effects of 3-HT on ROS generation and the MAPK signaling pathway. As shown in Fig. 5A and B, treatment with 3-HT at 2, 4 and 8 μM for 24 h demonstrated higher ROS levels compared with the control group in both cell lines. ROS levels increased by 1.19- (2 μM), 1.23- (4 μM), and 1.23- (8 μM)-fold by 3-HT over

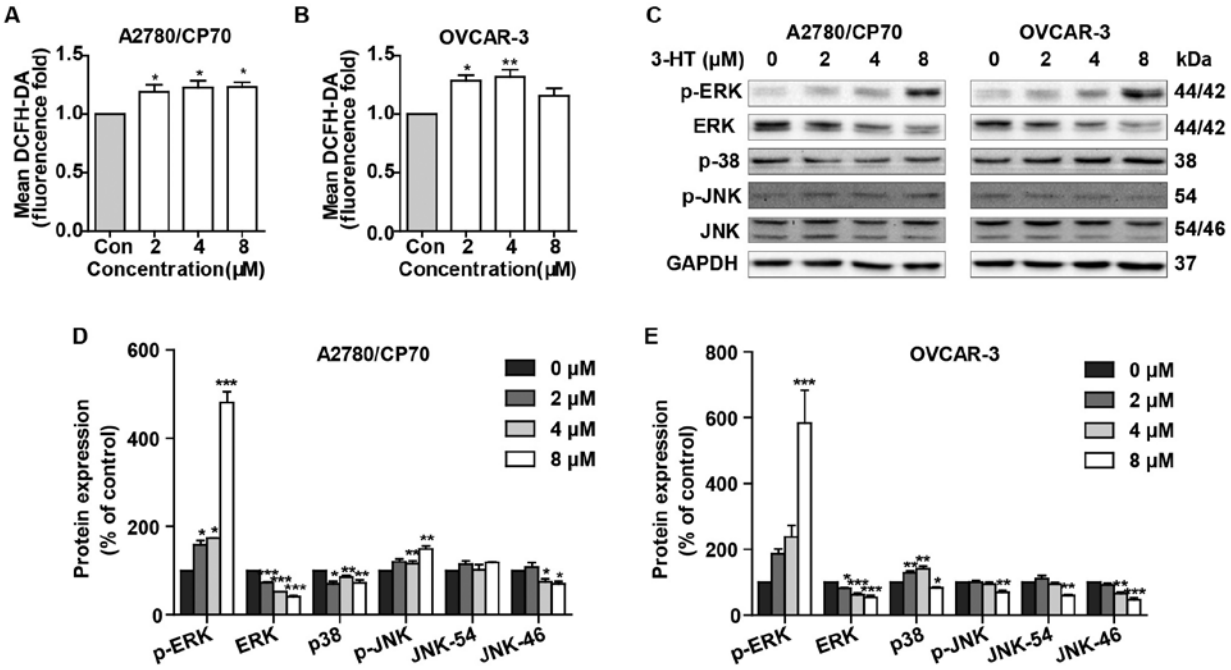

Figure 5. 3-HT induces ROS generation and activates the MAPK pathway. (A and B) ROS generation in A2780/CP70 and OVCAR-3 cells were detected using DCFH-DA. Cells were treated with 3-HT for 24 h, then incubated with DCFH-DA, fluorescence intensity was measured by fluorescence microplate reader. Data were expressed as mean ± SEM of three independent experiments. *P<0.05, **P<0.01. (C) Protein levels of MAPK family in A2780/CP70 and OVCAR-3 cells were analysed by western blotting. Cells were treated with 3-HT for 24 h, cell lysates were then prepared and subjected to western blotting to detect the protein levels, GAPDH was used as internal control. (D and E) A2780/CP70 and OVCAR-3 protein expression data were expressed as means ± SEM of three independent experiments. *P<0.05, **P<0.01, ***P<0.001.

that in control groups in A2780/CP70 cells (Fig. 5A). Similar results were obtained in OVCAR-3 cells, the ROS levels increased by 1.28- (2 μM), 1.32- (4 μM), and 1.15- (8 μM)-fold compared with control groups (Fig. 5B). These results suggested that 3-HT elevated ROS levels dose-dependently in ovarian cancer cells.

We then determined the effects of 3-HT on p38, c-Jun N-terminal kinase (JNK), and extracellular regular protein kinase (ERK), the three main proteins of MAKPs family. Results showed that 3-HT significantly induced activation of ERK1/2 (Fig. 5C-E). The protein level of p-38 decreased in A2780/CP70 cells, while it increased in OVCAR-3 cells (Fig. 5C-E). Also, p-JNK protein levels were increased in A2780/CP70 cells and decreased in OVCAR-3 cells (Fig. 5C-E). The protein level of total JNK was inhibited in both cell types (Fig. 5C-E).

3-HT induces apoptosis via intrinsic and extrinsic apoptotic pathways. The two best-understood apoptotic activation mechanisms are the intrinsic and the extrinsic pathways. Considering the fact that 3-HT induced apoptosis in both A2780/CP70 and OVCAR-3 cells, we next examined whether the intrinsic and/or extrinsic apoptotic pathways were/was involved in the apoptotic effect by western blotting. We first detected the intrinsic apoptotic pathway related proteins such as Puma, Bax, Bad, Bcl2, Bcl-xL and procaspase-9. Puma protein expression was significantly upregulated in A2780/CP70 and OVCAR-3 cells (Fig. 6A-C). The level of pro-apoptotic protein Bax remained unaffected in A2780/CP70 cells (Fig. 6A and B); however, it slightly decreased in OVCAR-3 cells (Fig. 6A and C). Another pro-apoptotic protein Bad showed no significant changes in either cell type (Fig. 6A-C). Anti-apoptotic proteins Bcl-2 and Bcl-xL were inhibited after treatment with 3-HT (Fig. 6A-C). The procaspase-9 protein level was also inhibited in both cell lines (Fig. 6A-C). These results suggested that the intrinsic apoptotic pathway was involved in 3-HT-induced apoptosis.

We further checked the expression levels of extrinsic apoptotic pathway related proteins. The levels of DR4 and Fas receptor increased in A2780/CP70 cells; however, no significant changes were observed in OVCAR-3 cells (Fig. 6D and F). FADD protein expression levels were downregulated. We also observed that protein levels of DR5 were upregulated significantly in A2780/CP70 and OVCAR-3 cells (Fig. 6D-F). The results above indicated that the extrinsic apoptotic pathway was also involved in 3-HT-induced apoptosis in ovarian cancer cells.

Discussion

The major problem facing current cancer research is the resistance of cancer to chemotherapy and molecularly targeted therapies (18). Resistance to platinum-based drugs continues to be a major factor leading to therapeutic failure for ovarian cancer (19). In the present study, we first investigated whether 3-HT, the metabolite isolated from *Aspergillus candidus*, could exhibit anticancer effects *in vitro*. Our results clearly demonstrate that 3-HT exhibited significant cell viability inhibition effect against ovarian cancer cells due to the induction of S phase arrest and apoptosis at low concentrations. The IC_{50} values of 3-HT for the growth of A2780/CP70 and OVCAR-3 cells were 5.77 and 6.97 μM, respectively. These results were consistent with previous reports that many metabolites of

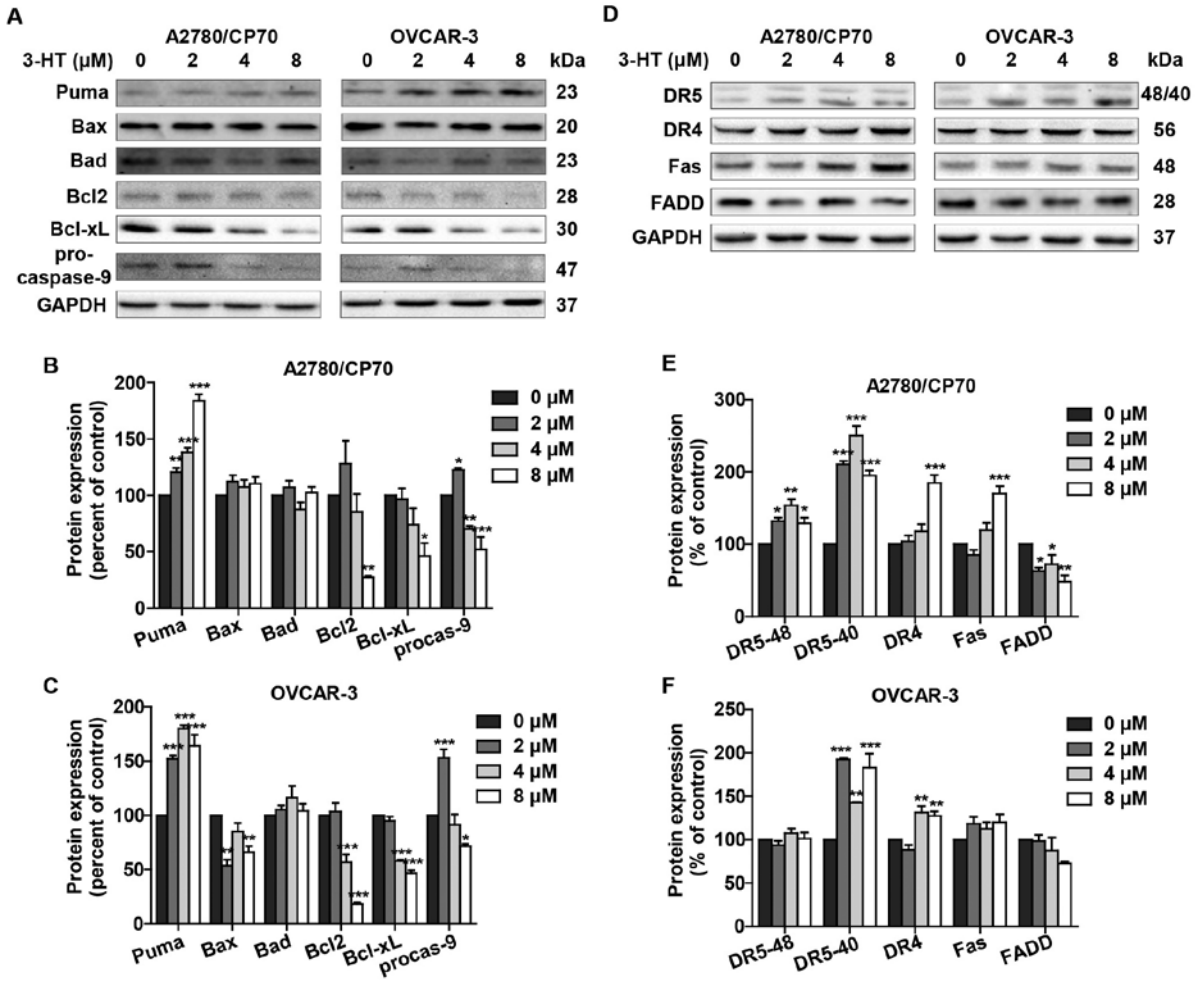

Figure 6. Effect of 3-HT on the intrinsic and extrinsic apoptotic pathways in A2780/CP70 and OVCAR-3 cells. (A) The intrinsic apoptotic related proteins were detected by western blotting. The cells were treated with 3-HT for 24 h. Cell lysates were prepared and then subjected to western blotting to detect the protein levels. GAPDH was used as internal control. (B and C) A2780 and OVCAR-3 protein expression data were expressed as means ± SEM of three independent experiments. *P<0.05, **P<0.01, ***P<0.001. (D) The intrinsic apoptotic related proteins were detected by western blotting. The cells were treated with 3-HT for 24 h. Cell lysates were prepared and then subjected to western blotting to detect the protein levels. GAPDH was used as internal control. (E and F) A2780/CP70 and OVCAR-3 protein expression data were expressed as means ± SEM of three independent experiments. *P<0.05, **P<0.01, ***P<0.001.

fungi inhibit cell proliferation in various cancer cell types (13,20,21). However, 3-HT also resulted in the loss of cell viability in IOSE-364. In LDH assay, significant alterations of LDH leakage levels were observed in both ovarian cancer cell lines while 3-HT caused slightly less LDH release in IOSE-364 cells. These results clearly suggested that 3-HT caused cytotoxic effects in both ovarian cancer cells. However, 3-HT was less cytotoxic to normal ovarian epithelial surface cells, IOSE-364. The MTS and LDH assays both suggested 3-HT demonstrated different effect on ovarian cancer cells and normal cells. Ideal anticancer drugs are expected to be cytotoxic to cancer cells while being selective towards normal cells with minimal cytotoxicity (22). The present study demonstrated the 3-HT selectivity towards ISOE-364 cells by increasing LDH release in A2780/CP70 and OVCAR-3 cells indicating targeted cytotoxicity. Cell cycle regulation plays an important role in tumorigenesis and tumor progression; thus, the molecules involved in cell cycle regulation become potential targets for therapeutic interventions (23). The eukaryotic cell cycle includes four sequential phases, G1, S, G2 and M. S and M phases are arguably the most pivotal phases pertaining to DNA replication and the creation of two new daughter cells (24). Flow cytometric analysis provided evidence that A2780/CP70 and OVCAR-3 cells were arrested at S phase after 3-HT treatment. Previous studies have shown that natural products and their derivatives are considered leads to the cell cycle pathway in cancer chemotherapy treatments (25). Some chemotherapy drugs like 5-fluorouracil and 6-mercaptopurine are commonly used to treat lukemias, ovarian and breast cancers, and other types of cancers by damaging cancer cells during the S phase (26). In addition, several other natural compounds, which have exhibited S phase arrest, have also been shown to induce apoptosis (27-29). In the present study, 3-HT reduced the cell viability of ovarian cancer cells partly through arresting cell cycle at S phase, thus, can become a candidate for further research to treat ovarian cancer in the future. Given the importance of the induction of apoptosis in cytotoxicity, we also evaluated the apoptotic effect of 3-HT on ovarian cancer cells using several methods. Nuclear chromatin condensation and nuclear DNA fragmentation are typical morphological hallmarks of apoptosis (30). These changes were clearly observed in both ovarian cancer cell lines after

treatment with 3-HT by Hoechst 33342 staining. Annexin V/PI staining further confirmed the number of apoptotic cells increased with increased concentrations of 3-HT. The loss of mitochondrial membrane potential is considered as another hallmark of early apoptosis. Our results showed a dose-dependent reduction of mitochondrial membrane potential in both cancer cell lines; thus, indicating that 3-HT induced apoptosis is related to mitochondrial damage. Protein cleavage is another key hallmark of apoptosis (31). The central role in the initiation of apoptosis is caspase-3 activation and the induction of cleavage of PARP by caspase-3 (32). In this study, the induction of caspase-3 and PARP cleavage indicated that 3-HT induced apoptosis was caspase-dependent. Collectively, all these results indicated that the anti-proliferation effect of 3-HT on ovarian cancer cells was also mediated by induction of apoptosis. Therefore, our results indicated that the anti-proliferative effects of 3-HT against ovarian cancer cells are correlated strongly with S phase arrest and apoptosis. To further elucidate the possible mechanisms that 3-HT induced cell cycle arrest at S phase, the expression of cell cycle regulatory proteins was determined by western blot analysis. Cyclin-dependent kinases (CDKs) are a family of protein kinases that regulate the cell cycle progression. 3-HT significantly inhibited the expression of cyclin E1, cyclin A2 and CDK2; thus, preventing the formation of cyclin E-CDK2 and cyclin A2-CDK2 complexes, which play pivotal role in the initiation and progression of the S phase (33), ultimately leading to S phase arrest. The results were in accordance with previous studies that natural compounds induced S phase arrest by inhibiting the expression of cyclin E, cyclin A2 and CDK in different types of human cancer cells (27,28). A previous study reported that h-PNAS-4 induced S phase arrest in ovarian cancer cells via activation of the Cdc25A-Cdk2-cyclin E/cyclin A pathway, the expression of cyclin E and cyclin A were upregulated while Cdc25A was inhibited (34). However, in this study, we found that Cdc25A was increased while cyclin E and cyclin A were inhibited. The inhibition of cyclin E and cyclin A prevented the formation of cyclin E/CDK2 and cyclin A/CDK2 complexes and leading to the S phase arrest. 3-HT downregulated the expression of CDK4 and cyclin D1, as cyclin D1 is only suppressed in S phase and its inhibition is an index for S phase arrest (34). The downregulation of cyclin D1/Cdk4 complex was also observed in a previous report in resveratrol-induced cell arrest in colon cancer cells (35). We thus, concluded that the downregulation of CDK4 and cyclin D1 contributed to the S phase arrest in A2780/CP70 and OVCAR-3 cells. Moreover, the upregulation of cyclin B1 induced by 3-HT was also observed in A2780/CP70 cells. Several reports also found an increase of cyclin B1 that was correspondent with the S phase arrest induced by different compounds in various cancer lines (36-38). These results indicated that 3-HT induced S phase arrest stemmed from the inactivation of cyclin E/Cdk2, cyclin A/Cdk2 and cyclin D1/Cdk4 complexes. The upregulation of cyclin B1 also contributed to the S phase arrest. Cell cycle arrest might be associated with the induction of DNA damage via activation of ATM/p53-mediated DNA damage response in MCF-7 cells (39). ATM is a DNA damage sensor that participates in the detection of DNA double-stranded breaks. Studies have indicated that ATM is activated when double-stranded breaks occur, and activated ATM results in the phosphorylation of p53 at Ser15 in response to DNA damage (40,41). ATM could also directly phosphorylate H2AX at Ser139, which is considered an early event in response to DNA damage (42). Chk1 and Chk2 are involved in channeling DNA damage signals from ATR and ATM in mammalian cells, respectively. Other research has shown that Chk2 at Thr68 is phosphorylated by ATM in response to DNA damage (43,44). Indeed, in the present study, 3-HT treatment led to the upregulation of p-ATM in A2780/CP70 cells. The DNA double strand breaks that occurred in A2780/CP70 and OVCAR-3 cells were indicated by the significant upregulation of γ-H2AX. Total p53 and phosphorylation of p53 at Ser15 were dramatically increased in both ovarian cancer cell lines; furthermore, a significant induction of p-Chk2 was observed in a dose-dependent manner in both A2780/CP70 and OVCAR-3 cells. We also observed significant inhibition of Cdc25C in both cancer cell types. A previous study has reported that the activation of the ATM/ATR-Chk1/2-Cdc25C pathway is a central mechanism in S phase arrest in OVCAR-3 cells induced by resveratrol (38). Our results strongly suggest this pathway was involved in the 3-HT induced S phase arrest in A2780/CP70 and OVCAR-3 cells.

The intrinsic and the extrinsic apopotic pathways are well documented. The intrinsic pathway is mediated by molecules released from mitochondria (45). Cytochrome *c* and AIF are released from the mitochondria to the cytosol, and caspase-9 is activated during the prosess (46). Caspase-9 plays a key role in the intrinsic pathway through activating caspase-3 and caspase-7 (47). In this study, procaspase-9 was decreased and cleaved caspase-3 was upregulated in both ovarian cancer cells indicating that 3-HT triggered the intrinsic apoptotic pathway. Bcl-2 family proteins are considered key regulators of the intrinsic pathway. The mitochondrial membrane permeabilization is governed by either pro-apoptotic (Puma, Bax, Bad and Bak) or anti-apoptotic (Bcl-2, Bcl-xL,Bcl-B and Bcl-W) proteins (48). Puma is a pro-apoptotic factor which served as a direct mediator of p53-associated apoptosis. The expression of Puma can induce apoptosis in human cancer cells (49). Puma can transduce death signals to mitochondria where it induces mitochondrial dysfunction and caspase activation by binding and inhibiting multidomain Bcl-2 family members (50). A previous report found that Puma initiates apoptosis partly through dissociating Bax and Bcl-xL (51). In this study, 3-HT treatment significantly upregulated the protein level of Puma and downregulated Bcl2 and Bcl-xL in both ovarian cancer cell lines. Together with the downregulation of procaspase-9 and activation of caspase-3, our results strongly suggested that the intrinsic apoptotic pathway was involved in 3-HT-mediated apoptosis. The extrinsic apoptotic pathway is triggered by binding death ligands of the tumor necrosis factor (TNF) family to death receptors (DRs) (52). Here, the protein level of Fas was upregulated in 3-HT-treated ovarian cancer cells; furthermore, 3-HT markedly upregulated the proteins levels of DR4 and DR5. Similar results were found in paclitaxel triggered apoptosis in prostate cancer cells through upregulation of DR4 and DR5 protein levels (53). Our results showed that the protein expression of FADD was downregulated in both ovarian cancer cell types. A previous study also observed upregulation of DR4 and downregulation of FADD in TRAIL-mediated apoptosis in prostate carcinoma LNCap

cells (51). These results indicated that the extrinsic apoptotic pathway was also involved in 3-HT-induced apoptosis. It has been reported that damaging anticancer agents can upregulate p53 proteins levels, which subsequently upregulate DR4 and DR5 expression (54,55). Our results found that 3-HT induced DNA damage and resulted in the upregulation of p53 as well as DR4 and DR5 in both ovarian cancer cell lines. The specific role of p53 in 3-HT induced apoptosis worth further investigation.

The accumulation of ROS is an early event connected with cancer cell apoptosis induced by DNA damage (56,57). Excessive ROS can induce apoptosis. Previous studies have indicated that ROS induced apoptosis is mediated by p38 MAPK, JNK and ERK activation (58,59). ERK is a signaling molecule that plays a key role in cell survival and differentiation and can be activated by extracellular stimuli such as DNA-damaging agents (23). In this study, we observed that 3-HT significantly increased ROS production. Exposure to 3-HT induced ERK1/2 phosphorylation in both ovarian cancer cell lines and resulted in the upregulation of p-JNK in A2780/CP70 cells. Similar results were reported in HEMA and TEGDMA induced apoptosis by the formation of ROS and activation of MAP-kinases ERK, JNK and p38 (58). ERK activation can result in S phase arrest and apoptosis in human pancreatic cancer cells (60). Previous reports have also shown that activation of ERK is likely playing a role in 2,3-DCPE-mediated S phase arrest in human colon cancer cells (23). In the present study, we did not elucidate the specific mechanism of ROS generation and ERK activation in 3-HT-induced apoptosis and S phase in ovarian cancer cells, but the results provide fundamental evidence for further underlying the role of ROS generation and ERK activation in apoptosis.

In summary, the present study indicated for the first time that 3-HT, the metabolite of *Aspergillus candidus*, significantly inhibits proliferation of A2780/CP70 and OVCAR-3 cells. 3-HT treatment caused DNA damage and cell cycle arrest in the S phase. The results also indicated that 3-HT induced cell apoptosis by activating both the intrinsic pathway and the extrinsic death receptor pathway. The generation of ROS and activation of ERK also play an important role in 3-HT induced anti-proliferation effect on ovarian cancer cells. Thus, this study demonstrated that 3-HT should be considered as an important anti-proliferative and pro-apoptotic agent for ovarian cancer and needs further investigation.

Acknowledgements

We thank Dr Kathy Brundage from the Flow Cytometry Core at the West Virginia University for providing technical help on apoptosis and cell cycle analysis. This research was supported by the NIH grants P20RR016477 from the National Center for Research Resources and P20GM103434 from the National Institute for General Medical Sciences (NIGMS) awarded to the West Virginia IDeA Network of Biomedical Research Excellence. The present study was also supported by the grant number P20GM104932 from NIGMS, a component of the National Institutes of Health (NIH) and its contents are solely the responsibility of the authors and do not necessarily represent the official view of NIGMS or NIH. This study was also supported by the COBRE grant GM102488/RR032138, the ARIA S10 grant RR020866, the FORTESSA S10 grant OD016165.

References

1. Hennessy BT, Coleman RL and Markman M: Ovarian cancer. Lancet 374: 1371-1382, 2009.
2. Jayson GC, Kohn EC, Kitchener HC and Ledermann JA: Ovarian cancer. Lancet 384: 1376-1388, 2014.
3. Wang J and Wu GS: Role of autophagy in cisplatin resistance in ovarian cancer cells. J Biol Chem 289: 17163-17173, 2014.
4. Newman DJ and Cragg GM: Natural products as sources of new drugs over the 30 years from 1981 to 2010. J Nat Prod 75: 311-335, 2012.
5. Evidente A, Kornienko A, Cimmino A, Andolfi A, Lefranc F, Mathieu V and Kiss R: Fungal metabolites with anticancer activity. Nat Prod Rep 31: 617-627, 2014.
6. Velkov T, Roberts KD, Nation RL, Thompson PE and Li J: Pharmacology of polymyxins: New insights into an 'old' class of antibiotics. Future Microbiol 8: 711-724, 2013.
7. Kobayashi A, Takemoto A, Koshimizu K and Kawazu K: p-Terphenyls with cytotoxic activity toward sea urchin embryos. Agric Biol Chem 49: 867-868, 1985.
8. Yen GC, Chang YC, Sheu F and Chiang HC: Isolation and characterization of antioxidant compounds from *Aspergillus candidus* broth filtrate. J Agric Food Chem 49: 1426-1431, 2001.
9. Yen GC, Chiang HC, Wu CH and Yeh CT: The protective effects of *Aspergillus candidus* metabolites against hydrogen peroxide-induced oxidative damage to Int 407 cells. Food Chem Toxicol 41: 1561-1567, 2003.
10. Fesik SW: Promoting apoptosis as a strategy for cancer drug discovery. Nat Rev Cancer 5: 876-885, 2005.
11. Fulda S: Targeting apoptosis for anticancer therapy. Semin Cancer Biol 31: 84-88, 2015.
12. Li B, Gao Y, Rankin GO, Rojanasakul Y, Cutler SJ, Tu Y and Chen YC: Chaetoglobosin K induces apoptosis and G2 cell cycle arrest through p53-dependent pathway in cisplatin-resistant ovarian cancer cells. Cancer Lett 356 (2 Pt B): 418-433, 2015.
13. Chen YF, Wang SY, Shen H, Yao XF, Zhang FL and Lai D: The marine-derived fungal metabolite, terrein, inhibits cell proliferation and induces cell cycle arrest in human ovarian cancer cells. Int J Mol Med 34: 1591-1598, 2014.
14. Li YX, Himaya SW, Dewapriya P, Zhang C and Kim SK: Fumigaclavine C from a marine-derived fungus *Aspergillus fumigatus* induces apoptosis in MCF-7 breast cancer cells. Mar Drugs 11: 5063-5086, 2013.
15. Zhou B-BS and Elledge SJ: The DNA damage response: Putting checkpoints in perspective. Nature 408: 433-439, 2000.
16. Bakkenist CJ and Kastan MB: DNA damage activates ATM through intermolecular autophosphorylation and dimer dissociation. Nature 421: 499-506, 2003.
17. Siliciano JD, Canman CE, Taya Y, Sakaguchi K, Appella E and Kastan MB: DNA damage induces phosphorylation of the amino terminus of p53. Genes Dev 11: 3471-3481, 1997.
18. Holohan C, Van Schaeybroeck S, Longley DB and Johnston PG: Cancer drug resistance: An evolving paradigm. Nat Rev Cancer 13: 714-726, 2013.
19. Galluzzi L, Senovilla L, Vitale I, Michels J, Martins I, Kepp O, Castedo M and Kroemer G: Molecular mechanisms of cisplatin resistance. Oncogene 31: 1869-1883, 2012.
20. Elaasser M, Abdel-Aziz M and El-Kassas R: Antioxidant, antimicrobial, antiviral and antitumor activities of pyranone derivative obtained from *Aspergillus candidus*. J Microbiol Biotechnol Res 1: 5-17, 2011.
21. Koul M, Meena S, Kumar A, Sharma PR, Singamaneni V, Riyaz-Ul-Hassan S, Hamid A, Chaubey A, Prabhakar A, Gupta P, *et al*: Secondary metabolites from endophytic fungus penicillium pinophilum induce ROS-mediated apoptosis through mitochondrial pathway in pancreatic cancer cells. Planta Med 82: 344-355, 2016.
22. Blagosklonny MV: Overcoming limitations of natural anticancer drugs by combining with artificial agents. Trends Pharmacol Sci 26: 77-81, 2005.

23. Zhu H, Zhang L, Wu S, Teraishi F, Davis JJ, Jacob D and Fang B: Induction of S-phase arrest and p21 overexpression by a small molecule 2[[3-(2,3-dichlorophenoxy)propyl] amino]ethanol in correlation with activation of ERK. Oncogene 23: 4984-4992, 2004.
24. Williams GH and Stoeber K: The cell cycle and cancer. J Pathol 226: 352-364, 2012.
25. Newman DJ, Cragg GM, Holbeck S and Sausville EA: Natural products and derivatives as leads to cell cycle pathway targets in cancer chemotherapy. Curr Cancer Drug Targets 2: 279-308, 2002.
26. Cheung-Ong K, Giaever G and Nislow C: DNA-damaging agents in cancer chemotherapy: Serendipity and chemical biology. Chem Biol 20: 648-659, 2013.
27. Liao Y, Ling J, Zhang G, Liu F, Tao S, Han Z, Chen S, Chen Z and Le H: Cordycepin induces cell cycle arrest and apoptosis by inducing DNA damage and up-regulation of p53 in leukemia cells. Cell Cycle 14: 761-771, 2015.
28. Lee YS, Choi KM, Kim W, Jeon YS, Lee YM, Hong JT, Yun YP and Yoo HS: Hinokitiol inhibits cell growth through induction of S-phase arrest and apoptosis in human colon cancer cells and suppresses tumor growth in a mouse xenograft experiment. J Nat Prod 76: 2195-2202, 2013.
29. Joe AK, Liu H, Suzui M, Vural ME, Xiao D and Weinstein IB: Resveratrol induces growth inhibition, S-phase arrest, apoptosis, and changes in biomarker expression in several human cancer cell lines. Clin Cancer Res 8: 893-903, 2002.
30. Hengartner MO: The biochemistry of apoptosis. Nature 407: 770-776, 2000.
31. Bratton SB and Cohen GM: Apoptotic death sensor: An organelle's alter ego? Trends Pharmacol Sci 22: 306-315, 2001.
32. Cohen GM: Caspases: The executioners of apoptosis. Biochem J 326: 1-16, 1997.
33. Eastman A: Cell cycle checkpoints and their impact on anticancer therapeutic strategies. J Cell Biochem 91: 223-231, 2004.
34. Yeo EJ, Ryu JH, Chun YS, Cho YS, Jang IJ, Cho H, Kim J, Kim MS and Park JW: YC-1 induces S cell cycle arrest and apoptosis by activating checkpoint kinases. Cancer Res 66: 6345-6352, 2006.
35. Wolter F, Akoglu B, Clausnitzer A and Stein J: Downregulation of the cyclin D1/Cdk4 complex occurs during resveratrol-induced cell cycle arrest in colon cancer cell lines. J Nutr 131: 2197-2203, 2001.
36. Zaffaroni N, Silvestrini R, Orlandi L, Bearzatto A, Gornati D and Villa R: Induction of apoptosis by taxol and cisplatin and effect on cell cycle-related proteins in cisplatin-sensitive and -resistant human ovarian cells. Br J Cancer 77: 1378-1385, 1998.
37. Wang CZ, Calway TD, Wen XD, Smith J, Yu C, Wang Y, Mehendale SR and Yuan CS: Hydrophobic flavonoids from Scutellaria baicalensis induce colorectal cancer cell apoptosis through a mitochondrial-mediated pathway. Int J Oncol 42: 1018-1026, 2013.
38. Tyagi A, Singh RP, Agarwal C, Siriwardana S, Sclafani RA and Agarwal R: Resveratrol causes Cdc2-tyr15 phosphorylation via ATM/ATR-Chk1/2-Cdc25C pathway as a central mechanism for S phase arrest in human ovarian carcinoma Ovcar-3 cells. Carcinogenesis 26: 1978-1987, 2005.
39. Lam M, Carmichael AR and Griffiths HR: An aqueous extract of Fagonia cretica induces DNA damage, cell cycle arrest and apoptosis in breast cancer cells via FOXO3a and p53 expression. PLoS One 7: e40152, 2012.
40. Abe K and Matsuki N: Measurement of cellular 3-(4,5-dimethylthiazol-2-yl)-2,5-diphenyltetrazolium bromide (MTT) reduction activity and lactate dehydrogenase release using MTT. Neurosci Res 38: 325-329, 2000.
41. Henkels KM and Turchi JJ: Cisplatin-induced apoptosis proceeds by caspase-3-dependent and -independent pathways in cisplatin-resistant and -sensitive human ovarian cancer cell lines. Cancer Res 59: 3077-3083, 1999.
42. Burma S, Chen BP, Murphy M, Kurimasa A and Chen DJ: ATM phosphorylates histone H2AX in response to DNA double-strand breaks. J Biol Chem 276: 42462-42467, 2001.
43. Ahn JY, Schwarz JK, Piwnica-Worms H and Canman CE: Threonine 68 phosphorylation by ataxia telangiectasia mutated is required for efficient activation of Chk2 in response to ionizing radiation. Cancer Res 60: 5934-5936, 2000.
44. Yuan Z, Guo W, Yang J, Li L, Wang M, Lei Y, Wan Y, Zhao X, Luo N, Cheng P, *et al*: PNAS-4, an early DNA damage response gene, induces S phase arrest and apoptosis by activating checkpoint kinases in lung cancer cells. J Biol Chem 290: 14927-14944, 2015.
45. Green DR: Apoptotic pathways: Paper wraps stone blunts scissors. Cell 102: 1-4, 2000.
46. Akasaka Y, Ito K, Fujita K, Komiyama K, Ono I, Ishikawa Y, Akishima Y, Sato H and Ishii T: Activated caspase expression and apoptosis increase in keloids: Cytochrome c release and caspase-9 activation during the apoptosis of keloid fibroblast lines. Wound Repair Regen 13: 373-382, 2005.
47. Ding H, Han C, Zhu J, Chen CS and D'Ambrosio SM: Celecoxib derivatives induce apoptosis via the disruption of mitochondrial membrane potential and activation of caspase 9. Int J Cancer 113: 803-810, 2005.
48. Brunelle JK and Letai A: Control of mitochondrial apoptosis by the Bcl-2 family. J Cell Sci 122: 437-441, 2009.
49. Yu J, Zhang L, Hwang PM, Kinzler KW and Vogelstein B: PUMA induces the rapid apoptosis of colorectal cancer cells. Mol Cell 7: 673-682, 2001.
50. Yu J and Zhang L: PUMA, a potent killer with or without p53. Oncogene 27 (Suppl 1): S71-S83, 2008.
51. Siddiqui IA, Malik A, Adhami VM, Asim M, Hafeez BB, Sarfaraz S and Mukhtar H: Green tea polyphenol EGCG sensitizes human prostate carcinoma LNCaP cells to TRAIL-mediated apoptosis and synergistically inhibits biomarkers associated with angiogenesis and metastasis. Oncogene 27: 2055-2063, 2008.
52. Sayers TJ: Targeting the extrinsic apoptosis signaling pathway for cancer therapy. Cancer Immunol Immunother 60: 1173-1180, 2011.
53. Nimmanapalli R, Perkins CL, Orlando M, O'Bryan E, Nguyen D and Bhalla KN: Pretreatment with paclitaxel enhances apo-2 ligand/tumor necrosis factor-related apoptosis-inducing ligand-induced apoptosis of prostate cancer cells by inducing death receptors 4 and 5 protein levels. Cancer Res 61: 759-763, 2001.
54. Wu GS, Burns TF, McDonald ER III, Jiang W, Meng R, Krantz ID, Kao G, Gan DD, Zhou JY, Muschel R, *et al*: KILLER/DR5 is a DNA damage-inducible p53-regulated death receptor gene. Nat Genet 17: 141-143, 1997.
55. Guan B, Yue P, Clayman GL and Sun SY: Evidence that the death receptor DR4 is a DNA damage-inducible, p53-regulated gene. J Cell Physiol 188: 98-105, 2001.
56. Rogalska A, Marczak A, Gajek A, Szwed M, Śliwińska A, Drzewoski J and Jóźwiak Z: Induction of apoptosis in human ovarian cancer cells by new anticancer compounds, epothilone A and B. Toxicol In Vitro 27: 239-249, 2013.
57. Zhang Y, Zheng S, Zheng JS, Wong KH, Huang Z, Ngai SM, Zheng W, Wong YS and Chen T: Synergistic induction of apoptosis by methylseleninic acid and cisplatin, the role of ROS-ERK/AKT-p53 pathway. Mol Pharm 11: 1282-1293, 2014.
58. Samuelsen JT, Dahl JE, Karlsson S, Morisbak E and Becher R: Apoptosis induced by the monomers HEMA and TEGDMA involves formation of ROS and differential activation of the MAP-kinases p38, JNK and ERK. Dent Mater 23: 34-39, 2007.
59. Zhang X, Wang X, Wu T, Li B, Liu T, Wang R, Liu Q, Liu Z, Gong Y and Shao C: Isoliensinine induces apoptosis in triple-negative human breast cancer cells through ROS generation and p38 MAPK/JNK activation. Sci Rep 5: 12579, 2015.
60. Yadav V, Varshney P, Sultana S, Yadav J and Saini N: Moxifloxacin and ciprofloxacin induces S-phase arrest and augments apoptotic effects of cisplatin in human pancreatic cancer cells via ERK activation. BMC Cancer 15: 581, 2015.